Roaa J. Mohammed
Jasim M. Mansoor
Asaad A. Kamil

Department of Physics,
College of Science,
University of Diyala,
Diyala, IRAQ

A Detailed Evaluation of Zn:Cu Co-Doping Impacts on the Performance of Nanostructured CdO Thin Films

This study focuses on the production and analysis of nanostructured CdO films co-doped with zinc (Zn) and copper (Cu) using the sol-gel spin coating technique. X-ray diffraction analysis revealed that these films have a cubic crystalline structure typical of CdO. Surface morphology showed that both the doping ratio and the type significantly influence the microstructure of the films. The presence of O, Cu, Cd, and Zn in the initial solution was confirmed. The absorbance values of the prepared samples exhibit a positive correlation with the Cu content. In addition, the energy gap values were shown to be dependent on the Zn:Cu ratio. Conductivity, measured via the Hall effect, increased notably with Cu doping up to a 10% ratio. The results demonstrate the impact of Zn:Cu co-doping on the structural, optical, and electrical properties of CdO films, indicating their potential for optoelectronic applications.

Keywords: Spin coating; Cadmium oxide; Energy gap; Nanostructures
Received: 29 January 2024; **Revised:** 25 March 2024; **Accepted:** 01 April 2024

1. Introduction

Owing to their unparalleled properties for various nanotechnology applications, transparent conducting oxides (TCOs) have garnered considerable technological and scientific interest [1-3]. Cadmium oxide (CdO) is a significant constituent of the transparent conductive oxide (TCO) group, garnering considerable contemporary interest because of its noteworthy electrical and optical characteristics. CdO is classified as an n-type semiconductor because of its notable electrical conductivity. In addition, it shows exceptional optical transparency within the visible spectrum. CdO possesses a direct band gap energy ranging from 2.2 to 2.7eV [4]. The characteristics of CdO films make them advantageous for several applications, including but not limited to smart windows, heat mirrors, gas sensors, phototransistors, and optical communications [5-10].

By doping CdO films with varying metallic ions, the morphological, optical, and structural properties of the films can be changed. The process of introducing ionic impurities into CdO films results in substantial modifications to the band structure and, so, the physical properties. The process of introducing ions with radii different from those of Cd^{2+} into CdO, known as doping, can be achieved by incorporating ions such as Mn, Pr, Al, Cr, Ce, Sn, and Gd, resulting in significant improvements in bandgap energies as well as morphological and structural properties [11-14]. Therefore, doping is typically associated with improving the electrical and optical characteristics of CdO films. The practice of employing two different dopant ions on a single CdO film, commonly referred to as double doping, is being investigated, has recently been seen to result in CdO films with unique properties [15-17].

Metal-organic chemical vapor deposition (MOCVD) [18], successive ionic layer adsorption and reaction (SILAR) method [19], spray pyrolysis [20], pulsed laser deposition [21], RF magnetron sputtering [22], chemical bath deposition [23], and sol–gel processes [24] have all been reported for CdO thin film deposition. The sol–gel spin coating method has several advantages, including simplicity, composition control, and homogeneity [25]. Sol-gel method Zn:Cu co-doped CdO films have not been reported in the literature, to the best of our knowledge. Therefore, this study focuses on assessing the effects of Zn and Cu co-doping on the morphological, structural, electrical, and optical characteristics of CdO films. Here, we present a detailed examination of the properties of nanostructured CdO thin films co-doped with Zn and Cu for the first time.

2. Experimental Work

Using the sol-gel spin coating method, we prepared pure and co-doped CdO thin films on glass substrates. Cadmium acetate $Cd(CH_3COO)_2{\cdot}2H_2O$, was dissolved in 10 ml of 2-methoxyethanol to form a 0.5M solution. Copper acetate $Cu(CH_3COO)_2{\cdot}2H_2O$ and zinc acetate $Zn(CH_3COO)_2{\cdot}2H_2O$ were added to this solution in varying Zn:Cu ratios (10% Zn, 7.5% Zn:2.5% Cu, 5% Zn:5% Cu, 2.5% Zn:7.5% Cu, 10% Cu) to create a homogeneous solution. Monoethanolamine (MEA) was then introduced to the stirred mixture to achieve the desired viscosity and stability. The mixture was heated at 75°C for 2 hrs while stirring. This process yielded a clear, light-yellow solution, which was then left to stand at room temperature for 24 hrs.

Earlier research has shown that solution anesthetics can improve the morphology, crystallization, and pore structure of spin-coated thin film electrodes [26]. Prior to depositing the solution onto the glass substrates by spin coating, the substrates were cleaned in an ultrasonic water bath with diluted detergents, acetone, 99% pure ethanol, and deionized water for 20 min, then dried with nitrogen gas and preheated in an oven at 75°C. The aged solutions were filtered through a 0.1µm filter to remove any agglomerated particles, ensuring standardized thin-film deposition by spin coating.

All samples were spin-coated at 3300 rpm for 35s onto soda-lime glass substrates. Each layer was covered with a 200 mL solution and dried for 15 min on a heated plate set to 200°C. This coating and drying process was repeated five times. Subsequently, the samples were annealed in a furnace at 475°C for 1 hour and gradually cooled to room temperature. The structural, morphological, optical, and electrical properties of the pure and co-doped CdO thin films were characterized using XRD, FE-SEM, UV-visible spectroscopy, and the Hall effect.

3. Results and Discussion

XRD analysis was conducted to investigate the influence of co-doping Cu with Zn on the crystalline structure and crystallite dimensions of CdO specimens.

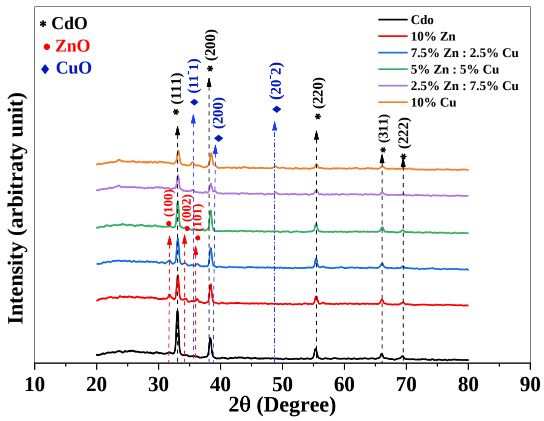

Fig. (1) XRD patterns of CdO and (Zn:Cu) co-doped thin films

The XRD patterns depicted in Fig. (1) prove that all the CdO samples show distinctive peaks associated with the cubic polycrystalline structure of CdO, as showed by ICDD card no. 75-0592. The presence of well-defined diffraction peaks indicates a high degree of crystallinity. The films co-doped with Cu and Zn show a pronounced preferential orientation along the (111) crystallographic plane, which is comparable to the orientation saw in the original CdO film. The Cu with Zn co-doped CdO films show markers associated with ZnO oxide and CuO oxide, which may be detected using an XRD setup with a specified detection limit. New peaks were seen in films having 10% Zn and 7.5% Zn:2.5% Cu, specifically corresponding to the (100), (002), and (101) planes of ZnO (ICDD 079-2205). Similarly, three peaks were shown in films having 10% Cu and 7.5% Cu:2.5% Zn, specifically corresponding to the $(11^{-}1)$, (200) and $(20^{-}2)$ planes of CuO (ICDD 080-1268). This implies that the successful incorporation of Cu and Zn ions into the CdO matrix was achieved [27]. A shift of 2θ toward higher diffraction angles is seen in the (111) diffraction, as depicted in Fig. (2). The observed phenomenon of a slight shift in the diffraction peak can be attributed to the presence of structural strain and changes in the stoichiometric composition resulting from the process of doping. The primary cause of this structural influence can be attributed to the disparity in the ionic radii between the host elements Cd^{+2} and the dopant ions Cu^{+2} and Zn^{+2}. Other researchers have also seen observed shifts in diffraction peaks when using other doping elements [28,29]. These findings show that a significant portion of Cu^{+2} and Zn^{+2} ions were integrated into the CdO lattice [30]. Moreover, the variability in the placement of the peaks shows that the lattice parameter undergoes alterations due to the disparity in the ionic sizes of the atoms [31].

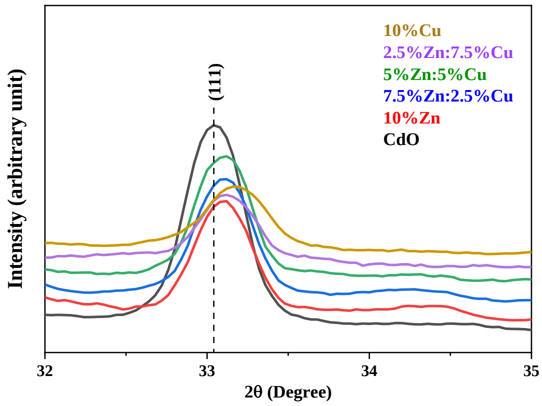

Fig. (2) XRD patterns of the preferential orientation of CdO and Zn:Cu co-doped CdO thin films

The crystallite sizes of the CdO thin films co-doped with Zn:Cu were determined using the widely recognized Scherrer's formula below [32]:

$$D = \frac{0.94\lambda}{\beta cos\theta} \quad (1)$$

In the given equation, the symbol D represents the dimension of the crystallite, β denotes the full-width at half maximum of the XRD peak, λ represents the wavelength of the x-ray (1.5406Å), and θ signifies the Bragg's angle. The calculation of additional microstructural parameters, including lattice spacing (d), lattice constant (a), strain (ε), and dislocation density (δ), can be achieved by the using of equations (2), (3), (4) and (5) [33,34]

$$d = \frac{n\lambda}{2dsin\theta} \quad (2)$$

$$\frac{1}{d^2} = \frac{h^2+k^2+l^2}{a^2} \quad (3)$$

$$\varepsilon = \frac{\beta cos\theta}{4} \quad (4)$$

$$\delta = \frac{1}{D^2} \quad (5)$$

In the context of XRD, the variable *n* denotes the degree of diffraction, λ indicates the wavelength associated with the XRD pattern, and θ signifies the diffraction angle. The values of D, ε, and δ that were acquired are displayed in table (1). The variations in the ε, D, and δ values of the CdO films are seen to be contingent on the different doping percentages of Cu:Zn, as depicted in table (1). The observed phenomenon can likely be attributed to the replacement of Cd^{+2} ions with Cu^{+2} or Zn^{+2} ions inside the CdO lattice structure. This substitution occurs because the ionic radii of Cu^{+2} (0.72Å) and Zn^{+2} (0.74Å) deviate from that of Cd^{+2} (0.97Å) when considering metals with a coordination number of 6 [35]. Several researchers have similarly reported these findings [36,37]. The literature clearly sets up a relationship between crystallite size, microstrain, and dislocation density, indicating an unfavorable correlation [38].

The analysis of surface morphology plays a crucial role in understanding the surface characteristics of nanostructured films. To investigate the alterations in the surface morphology of CdO films induced by double-doping, FE-SEM was performed as in Fig. (3) as the modification of the surface characteristics and particle dimensions of the films by the process of doping are proved. These images reveal that the surface of the CdO films showed a remarkable state of roughness. The CdO films are characterized by a significant quantity of nanoparticles that are spread in a random manner across the substrates made of soda-lime glass. The morphology of the pure CdO thin film shows a cauliflower-like shape, while the CdO thin films co-doped with Cu:Zn exhibit nanospherical granules. Earlier studies conducted by researchers [34] have also saw comparable structural characteristics in CdO films. Variations in the particle thicknesses of the films were seen upon co-doping with Cu and Zn, as depicted in Fig. (3). These changes showed a strong correlation with the variations in crystallite size, as determined by XRD analysis. The particle size values for the films of CdO, 10% Zn, 7.5% Zn:2.5% Cu, 5% Zn:5% Cu, 2.5% Zn:7.5% Cu, and 10% Cu are approximately 43.71-69.08nm, 37.07-101.5nm, 29.24-55.91nm, 36.43-267.1nm, 27.69-86.23nm, and 25.81-48.57nm, respectively.

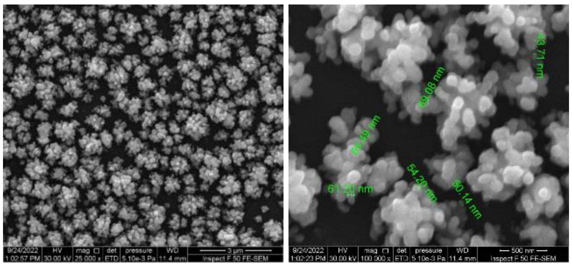
CdO

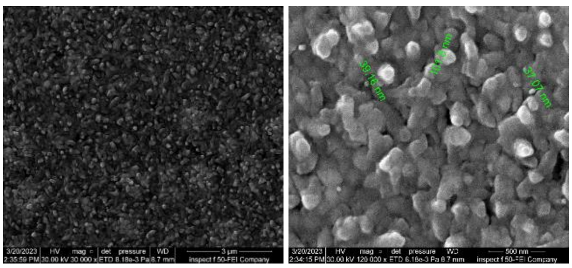
10% Zn

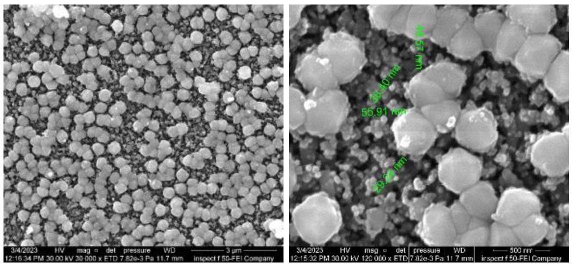
7.5% Zn:2.5% Cu

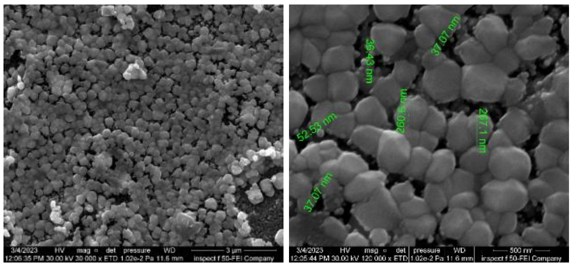
5%Zn:5%Cu

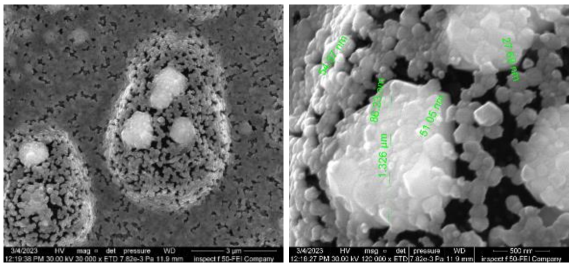
2.5% Zn:7.5% Cu

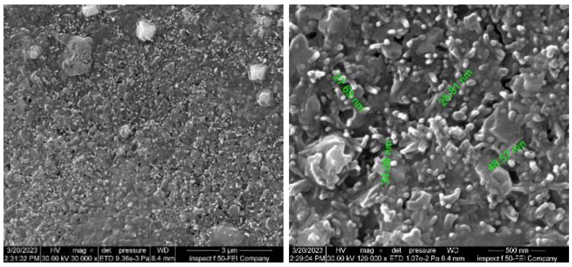
10% Cu

Fig. (3) FE-SEM images of the CdO and (Cu:Zn) co-doped CdO thin films

The variation in morphologies observed can be attributed to disparities in the electronegativity and ionic radius between the dopants and the host metal. These differences influence the growth process and the crystal plane surfaces of CdO films [35,36]. The researchers used the EDS analysis to find the elemental compositions of the samples that were generated. Figure (4) shows the elements in the nanostructured CdO films demonstrating the presence of the expected O, Cu, Cd, and Zn elements in the first solution.

The absorption spectra for the CdO thin films and 10% co-doped CdO thin films with varying Cu:Zn ratios (10%Zn, 2.5%Cu:7.5%Zn, 5%Cu:5%Zn, 7.5%Cu:2.5%Zn, and 10%Cu) are presented in Fig. (5). The spectra were recorded in the wavelength range of 300-900 nm. The figure demonstrates that the absorbance edge is consistently positioned at approximately 500 for all samples. Moreover, there is a discernible pattern in which the absorption spectrum demonstrates an upward trend as the ratio of copper to zinc increases. The presence of elevated copper content in the co-doped CdO films results in the generation of supplementary energy levels situated within the bandgap. The presence of these energy levels enables a more effective process of light absorption, leading to an amplification of the absorption spectrum. Consequently, the degree of absorbance of films becomes more prominent when the ratio of copper to zinc in the doping composition increases. The simultaneous incorporation of both copper (Cu) and zinc (Zn) dopants in co-doped CdO films results in a synergistic phenomenon. The introduction of Cu doping results in the incorporation of deep energy levels, while Zn doping functions as a donor of shallow levels. Variations in the optical characteristics of dual-doped CdO films can be attributed to the influence of the specific Cu:Zn ratio, which figures out the dominance of one effect over the other. The ability to customize the composition of CdO thin films by adjusting the percentages of Cu and Zn allows the optimization of these films for various applications in optoelectronics, sensors, and other electronic devices [39].

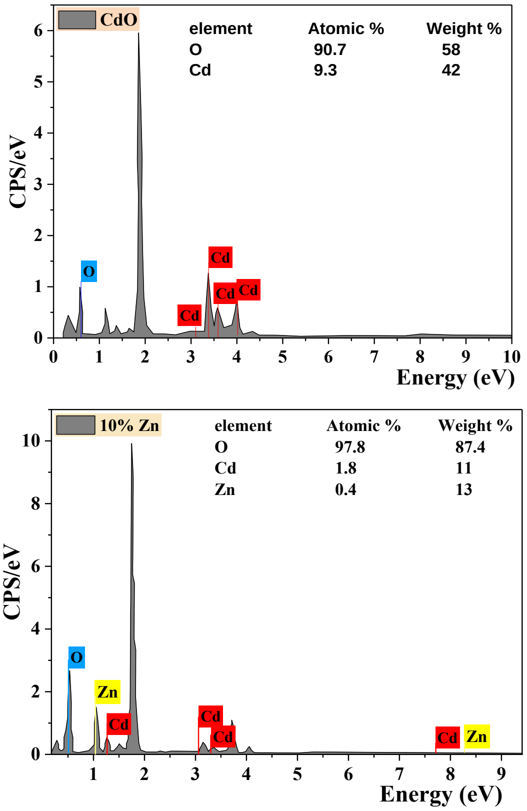

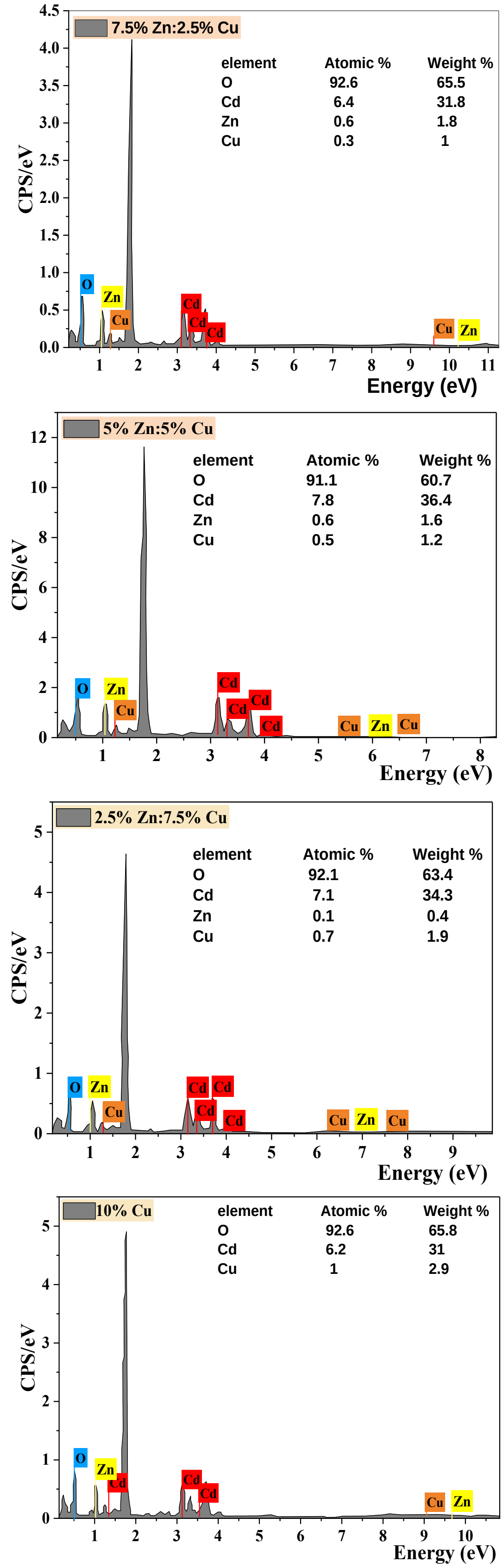

Fig. (4) EDS spectra of the prepared CdO and Zn:Cu co-doped CdO thin films

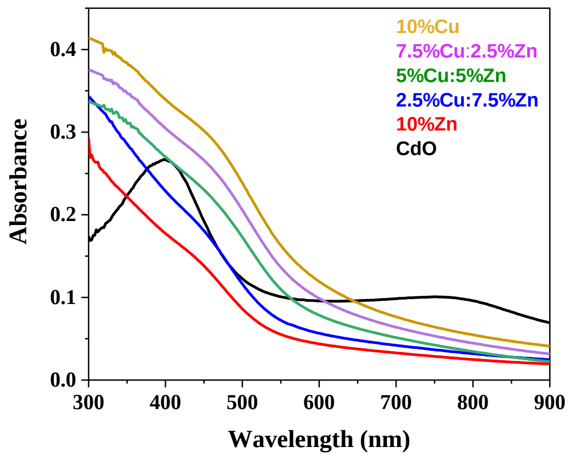

Fig. (5) Absorption spectrum of the CdO and Zn:Cu co-doped CdO thin films

The determination of the optical bandgap ($E_{g(opt)}$) for the thin films of dual-doped CdO with varying Zn:Cu ratios was performed using the Tauc formula below, described in reference [34].

$$\alpha h\nu = A(h\nu - E_g)^{1/2} \quad (6)$$

In the previous equation, α represents the coefficient of absorption, A denotes a constant, $h\nu$ represents the energy of the photon, and E_g signifies the optical energy gap

According to the data presented in Fig. (6), the energy bandgap of the 5% Cu:5% Zn composition sample was measured to be 2.57eV. Furthermore, it is noteworthy that when the Cu:Zn ratio increases, the energy bandgap experiences a modest drop, reaching a value of 2.45eV. Nevertheless, there was an observed rise in the energy bandgap to 2.92eV as the Zn content increased compared to Cu. The inclusion of copper (Cu) in the co-doped CdO films introduces supplementary energy levels within the bandgap.

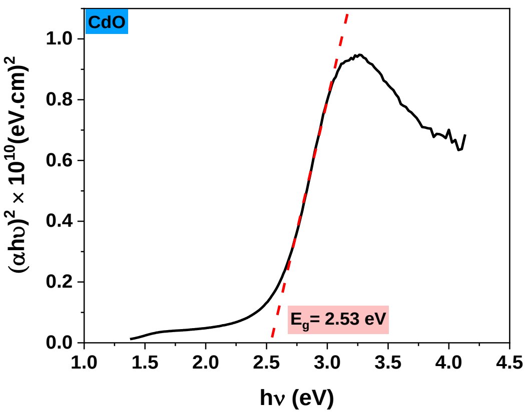

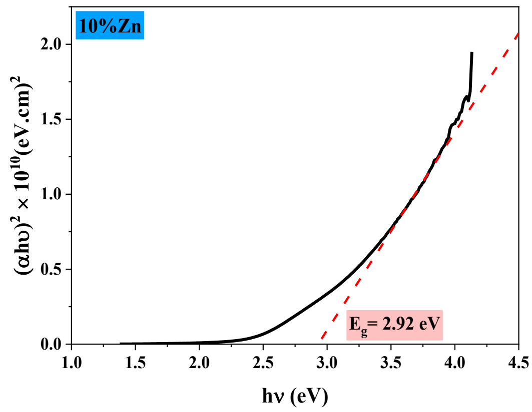

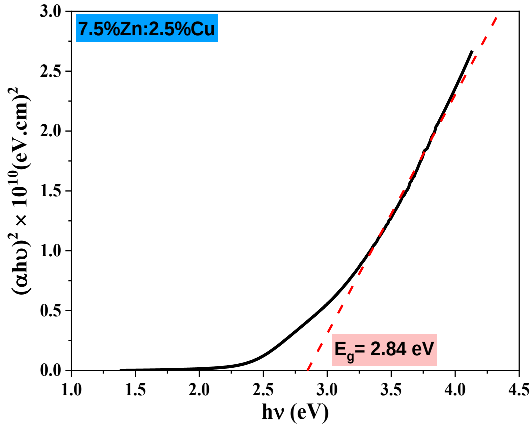

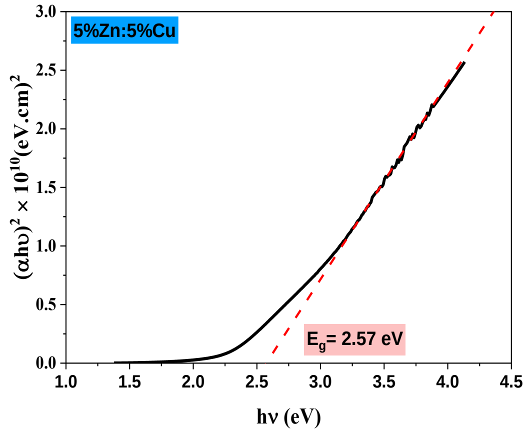

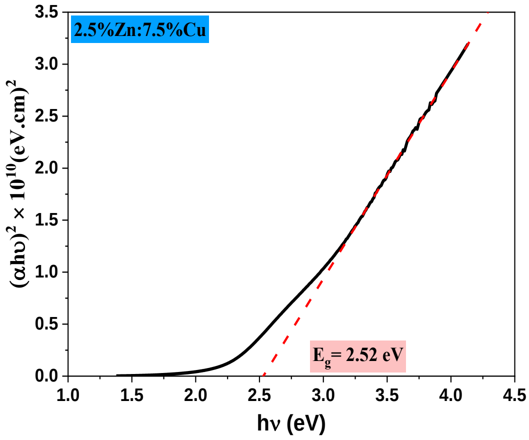

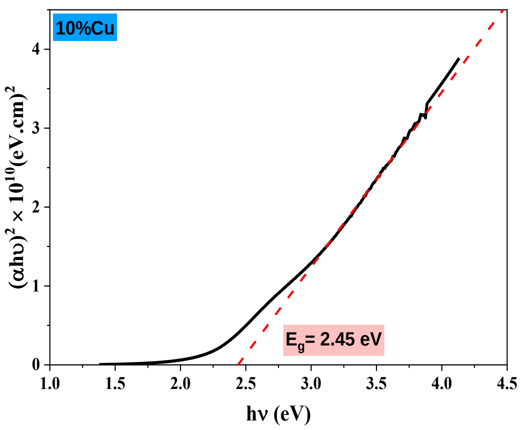

Fig. (6) Determination of optical band gap of CdO and Zn:Cu co-doped CdO thin films

The presence of deep energy states can confine electrons, resulting in a marginal drop in the energy necessary for absorption and thus a reduction in the optical bandgap. The Moss-Burstein effect has been identified as the underlying cause of the observed increase in the energy gap resulting from high-concentration doping with Zn [40]. The Moss-Burstein effect is characterized by the phenomenon of the absorption edge being displaced toward higher energy levels. The observed shift can be attributed to the filling of certain states next to the conduction band, which occurs when the concentration of electron carriers exceeds the density of available states. This phenomenon results in degenerating doping. In this phenomenon, once the concentration of electron carriers exceeds the density of states that are available states, all states found below the Fermi level become occupied. As a result, the excitation of electrons can solely occur within the conduction band, i.e., at energy levels surpassing the Fermi level. Consequently, the observed band gap can be expressed as the sum of the intrinsic band gap and the Moss-Burstein displacement [41]. This result aligns with the outcomes documented in the citation [42].

The use of Hall effect measurement is a helpful technique for introducing the fundamental electrical characteristics of metal oxide semiconducting materials, and hence assessing their appropriateness for certain applications [43]. Hall measurements were conducted at ambient temperature for thin films of CdO and Zn:Cu co-doped CdO deposited on glass substrates. The conductivity (σ), carrier concentration (n_H), and carrier mobility (μ_H) were figured out for each film sample, and the corresponding data are presented in table (2). The verification of the n-type conductivity of this system was set up through the observation of negative Hall coefficients in all thin layers. The occurrence of this phenomenon can be attributed to the existence of imperfections, including oxygen vacancies and/or intrinsic interstitial cadmium atoms, due to the strong likelihood of ionization associated with these defects. [44,45]. The electrons that are generated because of this process make a significant contribution to electrical conduction, hence causing CdO to show the characteristics of an n-type semiconductor. Based on the data presented in the table, the carrier concentration shows an upward trend as the percentage doping level increases. Conversely, the carrier concentration proves a downward trend as the percentage of Cu increases but experiences an upturn when the Cu content reaches 10%. Furthermore, the sample with a 10% Cu content exhibits the maximum level of conductivity.

The improvement in electrical properties observed for the co-doped CdO thin films can be attributed to the increase in carrier concentrations, mobilities, and conductivities, as well as the decrease in resistivity values. If Cu^{+2} and Zn^{+2} ions are replaced with Cd^{+2} ions or if Cu^{+2} and Zn^{+2} ions combine with O^{+2} ions, this improvement could occur. These techniques can enhance the carrier concentration of the deposited films by introducing an extra electron during every incorporation [46].

4. Conclusions

In conclusion, this research effectively produced CdO films doped with Zn and Cu using the sol-gel spin coating technique. The films show cubic crystalline structure. Significant changes in morphology and particle size were seen with Zn and Cu co-doping. Increasing Zn doping has raised the optical bandgap energy due to the Burstein-Moss effect, while increasing Cu doping lowered it. The n-type conductivity was confirmed in all films, with the highest conductivity saw at a 10% Cu doping level. These findings highlight the critical impact of dopant type and concentration on the CdO films' physical properties, especially the optical bandgap, pointing towards their potential in enhancing optoelectronic device technology.

Acknowledgements

This project received assistance from the Diyala University, College of Science.

References

[1] D. Sharma and R. Jha, "Transition metal (Co, Mn) co-doped ZnO nanoparticles: effect on structural and optical properties", *J. Alloys Comp.*, 698 (2017) 532-538.

[2] P.B. Nair et al., "Structural, optical, photoluminescence and photocatalytic investigations on Fe doped TiO2 thin films", *Thin Solid Films*, 550 (2014) 121-127.

[3] T. Jan, et al., "Structural, Raman and optical characteristics of Sn doped CuO nanostructures: a novel anticancer agent", *Ceram. Int.*, 41(10) (2015) 13074-13079.

[4] N. Manjula, et al., "Enhancement in some physical properties of spray deposited CdO: Mn thin films through Zn doping towards optoelectronic applications", *Optik*, 127(16) (2016) 6400-6406.

[5] R.N. Bulakhe and C.D. Lokhande, "Chemically deposited cubic structured CdO thin films: use in liquefied petroleum gas sensor", *Sens. Actuat. B: Chem.*, 200 (2014) 245-250.
[6] M. Ramamurthy, M. Balaji and P. Thirunavukkarasu, "Characterization of jet nebulizer sprayed CdO thin films for solar cell application", *Optik*, 127(8) (2016) 3809-3819.
[7] M. Soylu, A.A. Al-Ghamdi and F. Yakuphanoglu, "Transparent CdO/n-GaN (0001) heterojunction for optoelectronic applications", *J. Phys. Chem. Solids*, 85 (2015) 26-33.
[8] M. Eskandari, V. Ahmadi and R. Ghahary, "Enhanced photovoltaic performance of a cadmium sulfide/cadmium selenide-sensitized solar cell using an aluminum-doped zinc oxide electrode", *Ceram. Int.*, 41(2) (2015) 2373-2380.
[9] R.J. Deokate, et al., "Spray deposition of highly transparent fluorine doped cadmium oxide thin films", *Appl. Surf. Sci.*, 254(7) (2008) 2187-2195.
[10] E. Gürbüz, R. Aydin and B. Şahin, "A study of the influences of transition metal (Mn, Ni) co-doping on the morphological, structural and optical properties of nanostructured CdO films", *J. Mater. Sci.: Mater. Electron.*, 29 (2018) 1823-1831.
[11] Z. Ganjiani, F. Jamali-Sheini and R. Yousefi, "Electrochemical synthesis and physical properties of Sn-doped CdO nanostructures", *Superlatt. Microstruct.*, 100 (2016) 988-996.
[12] P. Velusamy et al., "Characterization of spray pyrolytically deposited high mobility praseodymium doped CdO thin films", *Ceram. Int.*, 42(11) (2016) 12675-12685.
[13] Z.A. Alahmed, et al., "Optical band gap controlling of nanostructure Mn doped CdO thin films prepared by sol–gel spin coating method", *Optik*, 126(5) (2015) 575-577.
[14] S. Aydemir, et al., "Influence of Al-doping on microstructure and optical properties of sol–gel derived CdO thin films', *Superlatt. Microstruct.*, 71 (2014) 72-81.
[15] N. Manjula and A.R. Balu, "Double doping (Mn+Cl) effects on the structural, morphological, photoluminescence, optoelectronic properties and antibacterial activity of CdO thin films", *Optik*, 130 (2017) 464-472.
[16] S. Akın, et al., "Improvement of physical properties of CdO thin films by Au–Ag nanocluster codoping", *J. Alloys Comp.*, 579 (2013) 272-278.
[17] R. Aydin and B. Şahin, "Comprehensive research on physical properties of Zn and M (M: Li, Na, K) double doped cadmium oxide (CdO) nanostructures using SILAR method", *Ceram. Int.*, 43(12) (2017) 9285-9290.
[18] D.A. Lamb and S.J. C. Irvine, "A temperature dependant crystal orientation transition of cadmium oxide films deposited by metal organic chemical vapour deposition", *J. Cryst. Growth*, 332(1) (2011) 17-20.
[19] B. Şahin, T. Taşköprü and F. Bayansal, "Bandgap variation of nanostructure tin doped CdO films via SILAR processing", *Ceram. Int.*, 40(6) (2014) 8709-8714.
[20] R. Kumaravel et al., "Electrical, optical and structural properties of aluminum doped cadmium oxide thin films prepared by spray pyrolysis technique", *Mater. Chem. Phys.*, 122(2-3) (2010) 444-448.
[21] B.J. Zheng et al., "Optical and electrical properties of Sn-doped CdO thin films obtained by pulse laser deposition", *Vacuum*, 85(9) (2011) 861-865.
[22] B. Saha, S. Das and K.K. Chattopadhyay, "Electrical and optical properties of Al doped cadmium oxide thin films deposited by radio frequency magnetron sputtering", *Sol. Ener. Mater. Sol. Cells*, 91(18) (2007) 1692-1697.
[23] R.R. Salunkhe, V.R. Shinde and C.D. Lokhande, "Liquefied petroleum gas (LPG) sensing properties of nanocrystalline CdO thin films prepared by chemical route: effect of molarities of precursor solution", *Sens. Actuat. B: Chem.*, 133(1) (2008) 296-301.
[24] F. Yakuphanoglu, "Synthesis and electro-optic properties of nanosized-boron doped cadmium oxide thin films for solar cell applications", *Sol. Ener.*, 85(11) (2011) 2704-2709.
[25] M. Thirumoorthi and J.T.J. Prakash, "A study of Tin doping effects on physical properties of CdO thin films prepared by sol–gel spin coating method", *J. Asian Ceram. Soc.*, 4(1) (2016) 39-45.
[26] G. Cerveau, R.J. Corriu and E. Framery, "Sol–gel process – influence of ageing on the textural properties of organosilsesquioxane materials", *J. Mater. Chem.*, 11(3) (2001) 713-717.
[27] M.A. Barakat, M. Shaban and A.M. El Sayed, "Structural, ultrasonic and spectroscopic studies of tin oxide thin films; effect of Ir and (Ni, Ir) double doping", *Mater. Res. Exp.*, 5(6) (2018) 066407.
[28] A.A. Dakhel, "Optoelectronic properties of Eu- and H-codoped CdO films", *Curr. Appl. Phys.*, 11(1) (2011) 11-15.
[29] R.J. Deokate, et al., "Structural, optical and electrical properties of chemically sprayed nanosized gallium doped CdO thin films", *J. Alloys Comp.*, 496(1-2) (2010) 357-363.
[30] A.A. Dakhel, "Correlated transport and optical phenomena in Ga-doped CdO films", *Sol. Ener.*, 82(6) (2008) 513-519.
[31] Y. Zhao et al., "The effect of Eu doping on microstructure, morphology and methanol-

sensing performance of highly ordered SnO_2 nanorods array", *Nanomater.*, 7(12) (2017) 410.

[32] I.S. Yahia et al., "Optical properties of Al-CdO nano-clusters thin films", Superlatt. Microstruct., 64 (2013) 178-184.

[33] N.K. Husien and J. Alzanganawee, "An investigation (Cd+Co) Co-Loading Impact on Physical Properties of Nano-Structured (CuO) Thin Films", *Acad. Sci. J.*, 1(1) (2023) 122-139.

[34] K.S. Mohammed et al., "An investigation of annealing and (Zn+Co) co-loading impact on certain physical features of nano-structured (CdO) thin films coated by a sol-gel spin coating process", *J. Ovonic Res.*, 17(5) (2021).

[35] R.D. Shannon, "Revised effective ionic radii and systematic studies of interatomic distances in halides and chalcogenides", *Acta Crystallog. A: Cryst. Phys. Diffract. Theor. Gen. Crystallog.*, 32(5) (1976) 751-767.

[36] C. Wang et al., "Structure, morphology and properties of Fe-doped ZnO films prepared by facing-target magnetron sputtering system", *Appl. Surf. Sci.*, 255(15) (2009) 6881-6887.

[37] A. Goktas et al., "Tuning of structural, optical and dielectric constants by various transition metal doping in ZnO: TM (TM= Mn, Co, Fe) nanostructured thin films: a comparative study", *Ceram. Int.*, 43(1) (2017) 704-713.

[38] P. Kumarn et al., "Nano porous hematite for solar hydrogen production", *J. Electrochem. Soc.*, 159(8) (2012) H685.

[39] B.A. Gozeh et al., "Zn-doped CdO effects on the optical, electrical and photoresponse properties of heterojunctions-based photodiodes", *J. Alloys Comp.*, 872 (2021)159624.

[40] N. Manjula et al., "Optoelectronic, magnetic and antibacterial properties of CdO thin films doubly doped with Mn (cationic) and F (anionic) ions", *J. Mater. Sci.: Mater. Electron.*, 28 (2017) 7615-7621.

[41] Z.M. Gibbs, A. LaLonde and G.J. Snyder, "Optical band gap and the Burstein–Moss effect in iodine doped PbTe using diffuse reflectance infrared Fourier transform spectroscopy", *New J. Phys.*, 15(7) (2013) 075020.

[42] I.S. Yahia et al., "Linear and nonlinear optical discussions of nanostructured Zn-doped CdO thin films", *Physica B: Cond. Matter*, 511 (2017) 54-60.

[43] S.A. Russell et al., "Surface transfer doping of diamond by MoO_3: A combined spectroscopic and Hall measurement study", *Appl. Phys. Lett.*, 103(20) (2013) 202112.

[44] S.J. Helen et al., "Transparent conducting Mo-doped CdO thin films by spray pyrolysis method for solar cell applications", *J. Electron. Mater.*, 47 (2018) 2439-2446.

[45] K. Sankarasubramanian et al., "Influence of substrate temperature on ethanol sensing properties of CdO thin films prepared by facile spray pyrolysis method", *J. Mater. Sci.: Mater. Electron.*, 26 (2015) 955-961.

[46] M. Anitha et al., "Influence of a novel co-doping (Zn+F) on the physical properties of nano structured (111) oriented CdO thin films applicable for window layer of solar cell", *Appl. Surf. Sci.*, 443 (2018) 55-67.

Table (1) Parameters of the CdO and Zn:Cu co-doped CdO thin films

Sample	2θ (deg)	FWHM (deg)	D (nm)	Lattice constant (a) (Å)	d-spacing (Å)	Strain (ε)	Dislocation density (δ) (nm^{-2})
CdO	33.0308	0.2430	35.6	4.6928	2.7097	0.001007	0.000789
10%Zn	33.1315	0.3493	24.8	4.6829	2.7017	0.001462	0.001626
7.5%Zn:2.5%Cu	33.0966	0.3143	27.5	4.6840	2.7045	0.001318	0.001322
5%Zn:5%Cu	33.1211	0.2396	36.1	4.6845	2.7025	0.001006	0.000767
2.5%Zn:7.5%Cu	33.1665	0.3143	27.5	4.6790	2.6989	0.001318	0.001322
10%Cu	33.2014	0.3492	24.8	4.6743	2.6962	0.001461	0.001626

Table (2) Carrier concentration, mobility, conductivity type of "CdO and Zn:Cu co-doped CdO thin films

Sample	$n\times10^{16}$ (cm^{-3})	μ_H (cm^2/v.sec)	σ_{RT} ($\Omega^{-1}.cm^{-1}$)	Type
CdO	-2.11	223	0.753	n-type
10%Zn	-31.40	75	3.75	n-type
7.5%Zn:2.5%Cu	-19.16	93	2.86	n-type
5%Zn:5%Cu	-13.02	110	0.61	n-type
2.5%Zn:7.5%Cu	-9.51	152	2.31	n-type
10%Cu	-30.82	127	6.26	n-type